energies

MDPI

Article

Cascade Active Balance Charging of Electric Vehicle Power Battery Based on Model Prediction Control

Qi Wang [1,2], Chen Wang [3], Xingcan Li [2] and Tian Gao [1,*]

[1] School of Electronic and Information, Northwestern Polytechnical University, Xi'an 710072, China
[2] School of Electronic Information Engineering, Xi'an Technological University, Xi'an 710032, China
[3] School of Electerical Engineering, Xi'an University of Technology, Xi'an 710048, China
* Correspondence: tiangao@nwpu.edu.cn

Abstract: As a bi-directional converter, the Buck-Boost converter, which has the advantages of simple structure and taking the SOC of the battery as the balance variable, is adopted as the balance topology in this paper. In view of the shortcomings of traditional balance topology, which can only balance two adjacent batteries, resulting in a long balance time and insufficient balance accuracy, a cascade active balance charging topology that can balance in intra-group and inter-group situations simultaneously is proposed. At the same time, the fuzzy control algorithm and model predictive control are used as the balance control strategies, respectively, to control whether the MOSFET is on or off in the balance topology circuit. The duty cycle is dynamically adjusted to the size of the balance current to achieve the balance of the battery pack. The results show that the cascade Buck-Boost balance topology based on model prediction control can accurately control the balancing current and improve the accuracy and speed of the balance, and it is more suitable for the actual working process.

Keywords: buck-boost converter; active balance charging; cascade balance topology structure; model predictive control; balance control strategy

check for updates

Citation: Wang, Q.; Wang, C.; Li, X.; Gao, T. Cascade Active Balance Charging of Electric Vehicle Power Battery Based on Model Prediction Control. *Energies* **2023**, *16*, 2287. https://doi.org/10.3390/en16052287

Academic Editor: Adolfo Dannier

Received: 25 December 2022
Revised: 13 February 2023
Accepted: 22 February 2023
Published: 27 February 2023

Copyright: © 2023 by the authors. Licensee MDPI, Basel, Switzerland. This article is an open access article distributed under the terms and conditions of the Creative Commons Attribution (CC BY) license (https://creativecommons.org/licenses/by/4.0/).

1. Introduction

As the core of electric vehicles, the performance of power batteries has become the main factor restricting the development of electric vehicles [1]. Due to the influence of factors such as the manufacturing process, storage environment, and ambient temperature during use, each battery in the battery pack will decay at different rates, resulting in differences between batteries and affecting the inconsistency of its performance [2,3]. Under dynamic working conditions, the consistency of battery pack deterioration is an inevitable process, which makes the battery's "effective energy storage" always lower than the "theoretical maximum energy storage" [4]. Therefore, how to equalize the whole power battery pack and make the SOC (State of Charge) state of each battery converge to the maximum extent is the key to prolonging the battery's service life, which is also the focus and difficulty of this research [5,6].

At present, research into battery balance technology mainly focuses on the balance topology structure and balance control strategy. Active balance charging based on a converter, which is a widely used balance topology, has the advantages of simple structure and reasonable cost, and its balance ability is not affected by the voltage difference between cells [7]. Xu et al., proposed a direct cell-to-cell balanced circuit based on LC resonant transformation [8], which can realize the direct and zero current switching balance of the cell with the highest voltage to the lowest voltage, and obtain high balance efficiency. However, this method can only achieve the balance between two cells at the same time, which is not suitable for large battery packs with many cells. However, this method can only achieve the balance between two cells at the same time, which is not suitable for large battery packs with many cells. J. Sahoo [9] have designed a balance topology based

on the Buck-Boost transformation, which can realize the simultaneous balance of any cells to any cells and has high balance efficiency and speed. However, a large number of switching switches are required, and there are problems such as large circuit volume, complex control, and low reliability. Therefore, the active equalization topology based on a converter is suitable for energy transfer between adjacent batteries [10,11]. When it is applied to a battery pack with many cells, it will lead to slow equalization speed and low equalization efficiency.

In terms of a balance control strategy, Wu designed an intelligent fuzzy balance control algorithm to balance the voltage of two adjacent single batteries [12]. Liao L proposed a battery equalization controller based on fuzzy control [13], and the designed balance scheme has the ability to maintain the equalized current between the cells in a series battery pack under different conditions. Wu T. et al. [14] designed a variable domain fuzzy control on the basis of DC/DC converters to improve the energy efficiency and time efficiency of the lithium battery balance system. Wang B. et al., studied the realization of balance control technology by combining neural networks with fuzzy controllers [15], and the team also proposed the PSO and the variable universe fuzzy control algorithm to control the battery balance [16]. However, these methods can only control the balance of two adjacent cells and do not consider the coordination of equalizers in the battery balance system from the perspective of global optimization [17].

Therefore, based on the Buck-Boost balance structure converter type, a cascade Buck-Boost balance topology is proposed in this paper, which improves the disadvantage that the traditional Buck-Boost circuit can only equalize two adjacent batteries. The cascade structure not only enables the cells of each layer to balance within the layer, but also can balance with other layers, and the balance speed and efficiency can be improved. At the same time, the model predictive control algorithm is applied to the balance control system. The inherent robustness of model predictive control is used to solve the uncertainty problem in dynamic working conditions, to obtain the minimum optimization performance in the finite time domain and to achieve the balance of the battery pack with the minimum number of energy transfers as the goal. The simulation and experimental results show that cascade active balance charging based on model prediction control can accurately control the balance current and improve the balance accuracy and speed, and it is more suitable for the actual working process.

2. Cascaded Active Balanced Topology

This paper uses a bi-directional Buck-Boost converter with a simple structure as a balance topology circuit. The speed of energy transfer is adjusted by adjusting the PWM duty cycle.

2.1. Principle of Operation

The cascade Buck-Boost balance topology adopts the hierarchical structure of the series battery pack. The adjacent single cells form a set of topologies, and the adjacent two groups form a new set of structures. As shown in Figure 1, B1 and B2, and B3 and B4, form a set of balanced structures, respectively, and B1 + B2 and B3 + B4 form a set of balanced structures, and so on.

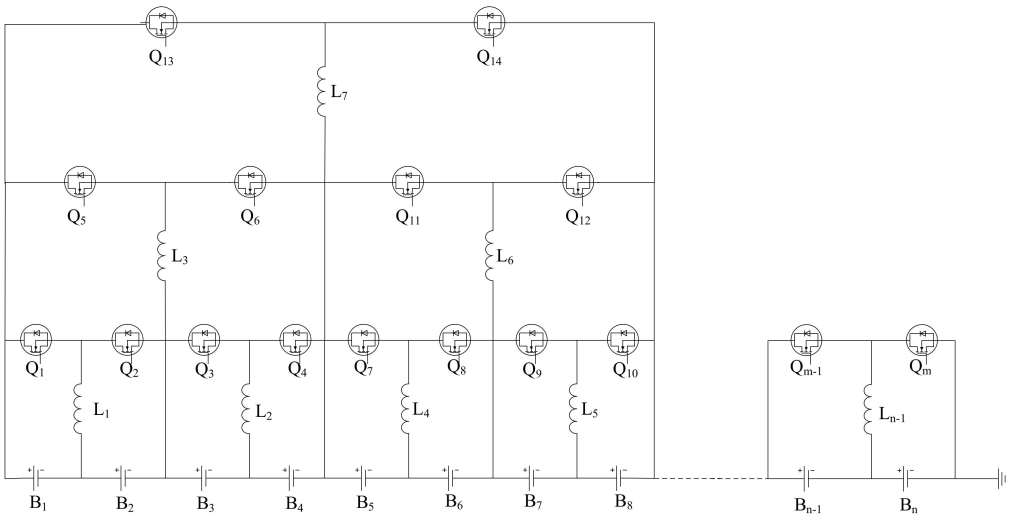

Figure 1. Cascaded Buck-Boost balance topology.

When the number of single cells is high, a ring-like structure is formed, which can be simultaneously balanced within and between groups, with multiple balanced circuits independent of each other.

Taking a four-cell single-cell series structure as an example, the cascaded Buck-Boost balance structure works as follows: Assume SOCB1 > SOCB2, SOCB4 > SOCB3, and SOCB1 + SOCB2 > SOCB3 + SOCB4.

In the inner ring, SOCB1 > SOCB2 allows Q1 to turn on and Q2 to disconnect, and at this time the single cell B1 to the energy storage inductance L1 charging; then, Q1 is disconnected, Q2 is turned on, and the inductance L1 charges the single cell B2. The two MOSFET driving signals of adjacent single cells complement each other and join the dead time at the same time. During the dead time, the inductor L1 continues to charge B2 by renewing the current through the anti-parallel diodes of B2 and Q2, which finally realizes the SOC balance of two adjacent single cells. Similarly, the balance between single cells B3 and B4 is achieved.

Meanwhile, in the outer ring, since SOCB1 + SOCB2 > SOCB3 + SOCB4 make it conductive and disconnect, Q1 and Q2 jointly charge inductor L3; then, this makes Q5 disconnect and Q6 conductive, at which time inductor L3 charges Q3 and Q4 simultaneously. The topology circuits of the outer and inner loops work simultaneously to achieve the balance of the four single cells.

In any ring, when the two adjacent cells' SOC values or the average SOC are detected as equal, the corresponding two switching tubes are disconnected. For example, when SOCB1 = SOCB2 is detected, Q1 and Q2 are disconnected at the same time, at which time B1 and B2 are equalized with other cells as a whole.

If the number of single cells on both sides of a set of the topology is inconsistent, the $\overline{\text{SOC}}$ values of the two batteries are compared to determine whether the balance is needed. If three single cells are equalized, a group of balanced circuits is formed between single cells B1 and B2, and a group of balanced circuits is formed between SOCB1 + SOCB2 and B3. When $\overline{\text{SOCB1}} + \overline{\text{SOCB2}} >$ SOCB3 meets the balance conditions, B1 + B2 (as a whole) and B3 are equalized.

2.2. Main Parameter Calculation of Balanced Topology Result

The frequency and duty cycle of the switching tube need to be taken into account because overcharging will saturate the inductor, resulting in an excessive inductor current. If the discharge time is short, then too little of the energy stored in the inductor is transferred, which will affect the balance speed of the battery pack. Therefore, the size of the inductance is the core of this scheme. The corresponding inductance can be calculated based on the control signal period and the maximum balance current.

The circuit works in the current discontinuous mode, to fully transfer the energy accumulated on the inductor and achieve zero energy accumulation. When the switch tube is turned on, part of the energy of the single cell will be stored in the inductance in the form of current, and the current in the inductance will increase linearly to the maximum value. The inductance current formula is as follows.

$$I(t) = \int_0^T \frac{U_b(t)}{L} dt \tag{1}$$

where U_b represents the battery terminal voltage, L represents the inductor, T represents the switching tube on-and-off cycle, duty cycle D is set no greater than 50%, and when the time is DT, the current on the inductor reaches its maximum value. The change of current on the inductor in one cycle can be expressed as:

$$I = \frac{U_b}{L} T \tag{2}$$

$$I_{\max} = \frac{U_b}{L} DT \tag{3}$$

Balanced circuit PWM control signal frequency f is set to 50 kHz, then the cycle T is 20 μs, the duty cycle is up to 45%, the balance maximum peak current is 2 A, and battery cell voltage up to 4.2 V, so each cycle to the inductor charging time is 9 μs and discharge time is 11 μs. Combining the above formulas, it can be derived that the inductor L is about 22 μH.

3. Balance Control Strategy of Power Battery Based on Model Prediction Control

To improve the balance speed and efficiency, the size of the balance current is dynamically adjusted according to the difference and mean value of the SOC between cells, which reduces the balance energy consumption and improves the balance efficiency.

3.1. Basic Principles of Model Prediction Control

The basic idea of model predictive control is to solve a finite time-domain open-loop optimization problem to obtain a control sequence based on the system state obtained from measurements at the current moment; however, only the first element of the control sequence is applied to the system, as shown in Figure 2 [18]. At the next moment, the process is repeated based on the new measured state. The online repetition of solving the open-loop optimization problem while predicting the time domain rolls forward to infinity. Closed-loop control is obtained by solving the relatively easy open-loop optimization problem. The process mainly consists of a prediction model, rolling optimization, and feedback correction.

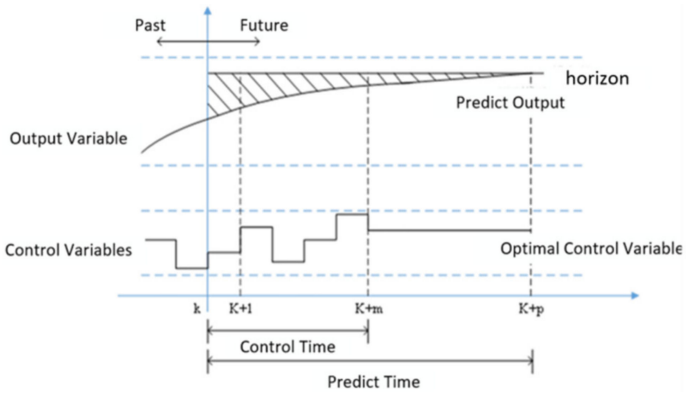

Figure 2. Model Predictive Control Schematic.

3.2. Balance Control Strategy Based on Model Prediction Control

The system dynamics model and the current SOC state of the battery are used to predict the state of the system and control the corresponding switching tubes for balance purposes. The difference between the SOC of each cell and the average value of the SOC of the series-connected battery pack is less than the set threshold in the shortest time.

3.2.1. Model Building

Assume that the battery pack of the balanced system is composed of n cells in series, with m balanced channels. The variables covered in this section are defined in Table 1.

Table 1. Variable Declaration.

Symbol of Variable	Meaning
τ	Battery self-loss rate
Q_C	Capacity of Section 1 to Section n of a single battery
T	Energy transfer of n series batteries and m equalization channels
Q_U	The maximum carrying current at equilibrium
Δt	Unit equalization time, related to the switching frequency of the MOSFET
x_n / X	SOC value of the battery
u_m / U	The balance current of each channel after normalization
k	Predicted step size

The n-dimensional state vectors $x = [x_1, x_2, x_3, \ldots, x_n]^T$ and $u = [u_1, u_2, u_3, \ldots, u_m]^T$ represent the SOC of n individual cells in the battery pack and the balance current after normalization, in which the balance current represents the current supplied by the l-th balanced circuit to the i-th individual cell.

The system input is the SOC of each battery, and the output is the balance current. The number of the input is equal to the number of batteries, and the number of outputs is equal to the number of balanced circuits.

The standard state-space model expression of the balanced system is expressed as:

$$\begin{cases} \dot{x} = Ax + Bu \\ y = Cx \end{cases} \tag{4}$$

In Equation (4), A, B and C are all $n \times n$ matrices, as shown in Equations (5) and (6).

$$A = (1 - \tau) I_{n*n} \tag{5}$$

τ describes the self-loss rate of the battery and takes a very small value. When $\tau = 0$, it means that the self-loss of the battery is neglected in the balance process. $I_{n \times n}$ means $n \times n$ unit matrix.

$$B = Q_C^{-1} T Q_U \Delta t \tag{6}$$

Q_C is a diagonal matrix representing a single cell's capacity from *1* to n.

$$Q_C = \begin{bmatrix} C_1 & 0 & \cdots & 0 \\ 0 & C_2 & \cdots & 0 \\ \vdots & \vdots & \ddots & \vdots \\ 0 & 0 & \cdots & C_n \end{bmatrix} \in R^{n \times n} \tag{7}$$

T represents the relationship between n series batteries and m balanced channels to describe the transfer amount during balance in a series battery pack. K represents the number of equalization layers, and the specific matrix form is selected according to the number of battery equalization segments. In the design matrix, it is also necessary to ensure that the sum of battery equalization coefficients in each column is 0. Where $T \in R^{n \times m}$, the

balanced transfer matrix T is written according to the modified Buck-Boost balance circuit, as follows.

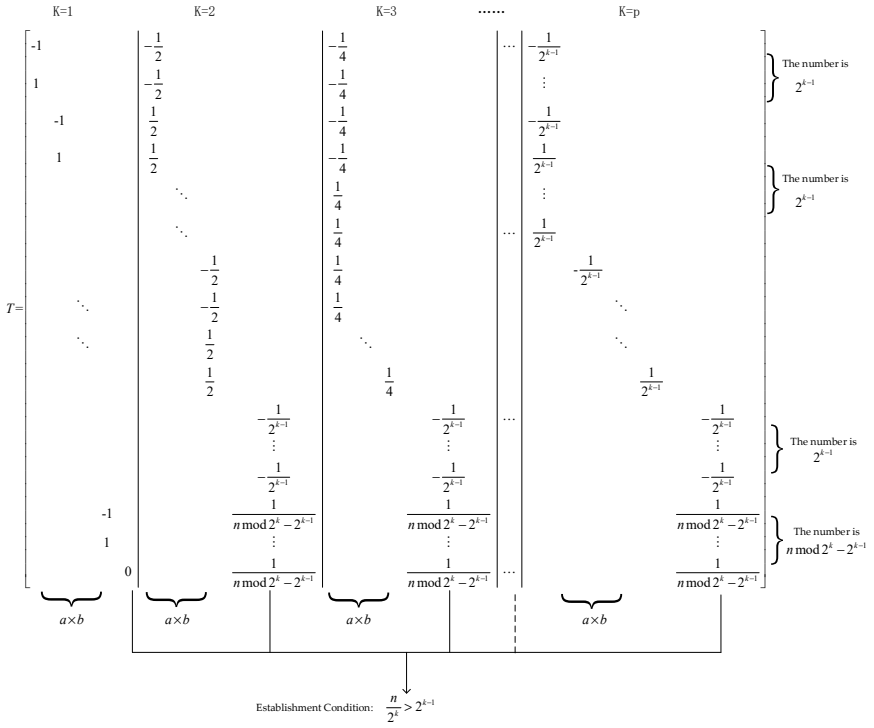

(8)

Among them, $a = 2^k \times \left[\frac{n}{2^k}\right]$,$b = \left[\frac{n}{2^k}\right]$.

Q_u represents the maximum balance current from channel *1* to channel m, in which $m = 2(n-1)$. $u = [u_1, u_2, u_3, \ldots, u_m]^T$ represents the balance current of each channel after normalization, and the actual balance current can be expressed as:

$$Q_U * u(t) \in R^{m \times 1} \tag{9}$$

Among them,

$$Q_U = \begin{bmatrix} I_1 & 0 & \cdots & 0 \\ 0 & I_2 & \cdots & 0 \\ \vdots & \vdots & \ddots & \vdots \\ 0 & 0 & \cdots & I_m \end{bmatrix} \in R^{m \times m} \tag{10}$$

Δt represents the unit balanced time, related to the switching frequency of the MOSFET.$u(t)$ indicates the current battery status. $u(t) > 0$ means to charge the battery, $u(t) < 0$ means to discharge the battery, and $u(t) \in \left\{ u \in R^{m \times 1} \middle| -1 \le u \le 1 \right\}$ means that the balance current of each channel is limited. $C = I_{n \times n}$, y represents the SOC state change.

$$\begin{cases} x(k) = A_1 x(k-1) + B_1 u(k-1) \\ y(k) = C_1 x(k-1) \end{cases} \tag{11}$$

where, t_0 is the sampling time, $A_1 = I_{n \times n} + At_0$, $B_1 = Bt_0$ and $C_1 = Ct_0$.

For discrete systems, the balance ends when the final state of the balance satisfies Equation (12).

$$x_1(K) = x_2(K) = \ldots x_n(K) \tag{12}$$

To further explain the process, take the discharge of four batteries. Where $n = 4$, $m = 3$, and $K = 2$, the current *T-matrix* can be obtained as:

$$T = \begin{bmatrix} -1 & 0 & -\frac{1}{2} \\ 1 & 0 & -\frac{1}{2} \\ 0 & -1 & \frac{1}{2} \\ 0 & 1 & \frac{1}{2} \end{bmatrix} \tag{13}$$

Then, we can obtain the B matrix, which is the balance change amount of the SOC.

$$B = \begin{bmatrix} -I_1 & 0 & -\frac{1}{2}I_3 \\ I_1 & 0 & -\frac{1}{2}I_3 \\ 0 & -I_2 & \frac{1}{2}I_3 \\ 0 & I_2 & \frac{1}{2}I_3 \end{bmatrix} \Delta t Q_C^{-1} \tag{14}$$

From the Equations (13) and (14), we can see that the current I_1 in channel 1 balanced battery 1 and 2; the current I_2 in channel 2 balanced battery 3 and 4; and the current I_3 between the two channels also completes the balance between channels.

However, Equation (12) can only be taken as an ideal state because of factors such as the acquisition error in the balanced system and the inefficiency of the balance transfer between the monomers.

The battery balance problem can be converted into a problem of minimizing the value of the battery SOC difference $\left|\left|x(k) - \overline{x(k)}\right|\right|$, which denotes the average value of battery SOC; therefore, the objective function is set as (13).

$$\min \sum_{i=0,k=0}^{i=n,k=K-1} (x_i(k) - \overline{x(k)}) \tag{15}$$

The balanced end threshold is set to $y(t) = \left|\left|x(k) - \overline{x(k)}\right|\right| \leq 0.5\%$, which uses the L2 norm. The expression that outputs y(t) is as follows:

$$y(t) = \begin{bmatrix} \frac{x_1+x_2+\ldots+x_n}{n} - x_1 \\ \frac{x_1+x_2+\ldots+x_n}{n} - x_2 \\ \vdots \\ \frac{x_1+x_2+\ldots+x_n}{n} - x_n \end{bmatrix} = \begin{bmatrix} \frac{1}{n} - 1 & \frac{1}{n} & \cdots & \frac{1}{n} \\ \frac{1}{n} & \frac{1}{n} - 1 & \cdots & \frac{1}{n} \\ \vdots & \vdots & \ddots & \vdots \\ \frac{1}{n} & \frac{1}{n} & \cdots & \frac{1}{n} - 1 \end{bmatrix} \begin{bmatrix} x_1 \\ x_2 \\ \vdots \\ x_n \end{bmatrix} \in R^{m \times m} \tag{16}$$

System constraints are (17).

$$\begin{gathered} \min J(x(k), \Delta u(k), m, n) \\ s.t. \begin{cases} 0 \leq x(k+1) \leq 1 \\ \overline{L}u(k) = 0 \\ |u(k)| \leq 1 \end{cases} \end{gathered} \tag{17}$$

Among them, $k = 1, 2, \cdots K$, $L = [1, -1, 1, -1, \ldots, 1, -1]_{1 \times m}$.

x(k + 1) because the SOC is between 0 and 1; $\overline{L}U(k) = 0$ because we expect the current of each channel to be 0 after equalization; u represents the normalized current magnitude, and absolute value is used to consider the direction.

The linear MPC design uses quadratic optimization, including the cost functions ${x_k}'Q x_k$ for state variables and ${u_k}'R u_k$ for control variables.

$$J_{(k,N)} = \min \sum_{t=k} ({x_t}'Q x_t + {u_t}'R u_t) \tag{18}$$

At time t, the optimization objective function of the rolling horizon step is N, and the purpose is to make the state quantity x and the control quantity u as small as possible. It can be achieved by using the least amount of energy to stabilize the system state quantities to zero as soon as possible.

3.2.2. Rolling Optimization

The rolling time-domain method replaces the future state variables and controls the balanced system. The predictive state expression of the balanced system is (19).

$$\begin{bmatrix} y(k+1|k) \\ y(k+2|k) \\ \vdots \\ y(k+N|k) \end{bmatrix} = \begin{bmatrix} A \\ A^2 \\ \vdots \\ A^N \end{bmatrix} y(k) + \begin{bmatrix} B(k|k) & 0 & \cdots & 0 \\ AB(k|k) & B(k+1|k) & \cdots & 0 \\ \vdots & \vdots & \ddots & \vdots \\ A^{N-1}B(k|k) & A^{N-2}B(k+1|k) & \cdots & B(k+N-1|k) \end{bmatrix} \begin{bmatrix} u(k|k) \\ u(k+1|k) \\ \vdots \\ u(k+N-1|k) \end{bmatrix} \tag{19}$$

System constraints are (20)–(22).

$$0 \le Y(k+1) \le 1 \tag{20}$$

$$\overline{L}U(k) = 0 \tag{21}$$

$$|U(k)| \le 1 \tag{22}$$

Among them, $\overline{L} = diag\{L_1, L_2, \ldots, L_N\}$. The future state quantities after the transformation are substituted into the optimization objective and can be solved. Replace the optimization objective function with all expressions about the optimization objective u_t and the current state y_k.

$$J_{(K,N)} = \min Y'\widetilde{Q}Y + U'\widetilde{R}U \tag{23}$$

Y represents the predicted battery SOC, as shown on the left of Equation (19). U represents the output balance current, as shown on the right of Equation (19).

$\widetilde{Q}$ and $\widetilde{R}$ are the optimized cost coefficient matrices after augmented transformation. The quadprog function is used for quadratic optimization in MATLAB.

$$[y, fval, exitflag] = quadprog(H, f, A, b, Aeq, beq, lb, ub, y_0, options) \tag{24}$$

$$\min_y \frac{1}{2} y'Hy + f'x \tag{25}$$

$$s.t. \begin{cases} Ay \le b \\ Aeq * y = beq \\ lb \le y \le ub \end{cases} \tag{26}$$

The quadprog function converts the optimization equation into a standard quadratic form for solution, as shown in Equation (25). The function is to find the magnitude of the required equalization current when the difference between the battery SOC and the average value of the whole group SOC is close to 0.

Substituting *x(t)* into the expression yields.

$$\begin{aligned} J_{(K,N)} &= (\widetilde{A}y_k + \widetilde{B}U)'Q_t(\widetilde{A}y_k + \widetilde{B}U) + U'R_tU \\ &= U'(\widetilde{B}'Q_t\widetilde{B} + R_t)U + 2y_k'\widetilde{A}'\widetilde{Q}\widetilde{B}U + y_k'\widetilde{A}'\widetilde{Q}\widetilde{A}y_k \end{aligned} \tag{27}$$

U is the optimization objective, and the third term is not related to the optimization objective, so it can be omitted.

$$H = 2(\widetilde{B}'\widetilde{Q}\widetilde{B} + \widetilde{R}) \tag{28}$$

$$f = (2y_k'\widetilde{A}'\widetilde{Q}\widetilde{B}) \tag{29}$$

The flow chart of the balance control strategy and the model prediction process is shown in Figure 3. First, the SOC value of each battery is obtained. Secondly, it is judged

whether the SOC difference between adjacent batteries is greater than 0.5%. When the difference is greater than 0.5%, model predictive control is used to balance the batteries. The specific method is the output SOC value of each moment under N steps, and the SOC value of the first step is taken as the return value. Then, the output SOC value is constantly corrected by controlling the equalization current.

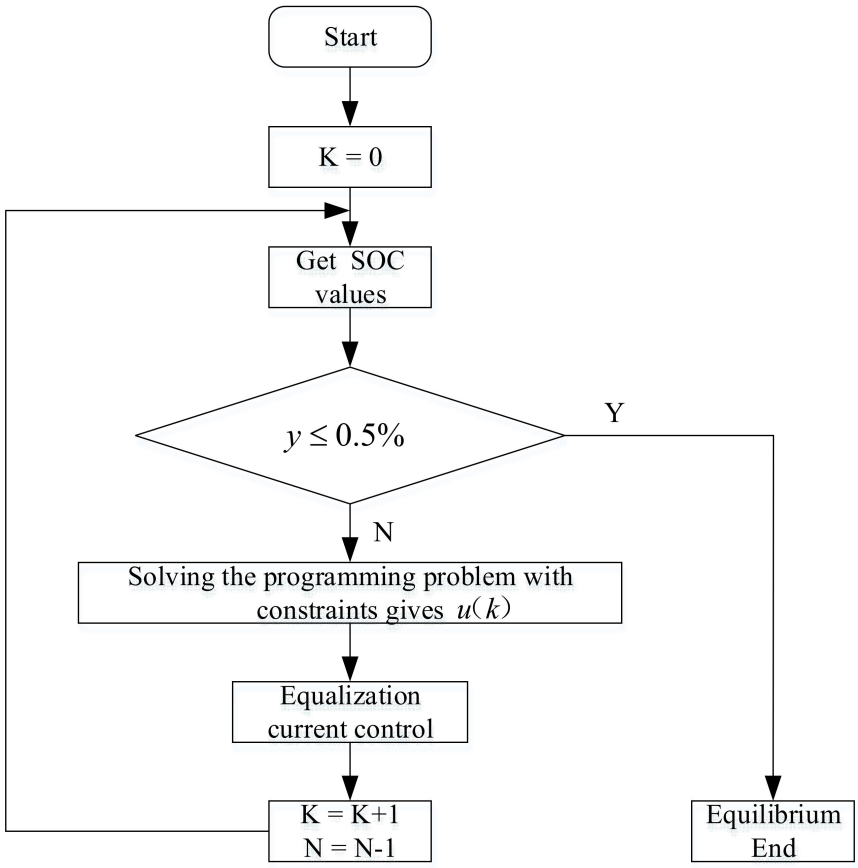

Figure 3. Flow chart of the balance control strategy.

The size of the balance current is achieved by controlling the duty cycle of the MOSFET. The duty cycle is calculated by first calculating the difference between the current inductor current and the current obtained by the MPC, and then dividing the difference by the maximum current the inductor can carry to obtain the duty cycle required. This method can quickly change the value of the balance current.

4. Experiments and Result Analysis

The static balancing of four series batteries, ignoring the battery self-discharge effect with a short time, and online access to the SOC value, are the balanced quantitative indicators of the balance control strategy and the input variables of the balance system. The initial values of SOC of every single cell were set to 51.5%, 50.5%, 49.5%, and 48.5% under the condition of battery resting, and other related parameters were as shown in Table 2.

Table 2. Relevant parameters in the balance control design.

Category	Value
Battery Capacity Qc	2600/mAh
Nominal Voltage V	3.7/V
Maximum Balanced Current I	2/A
Balanced Inductance L	22/μH
Switching Frequency f	50/KHz
Maximum Duty Cycle D	45%
Sampling Time t	1/s
Balanced Objective	0.5%

Four single batteries were connected in series to the cascade Buck-Boost balance topology based on fuzzy control and model prediction control for simulation. Figures 4 and 5 show the simulation results, where the abscissa represents the equalization time and the ordinate represents the SOC value of the single battery.

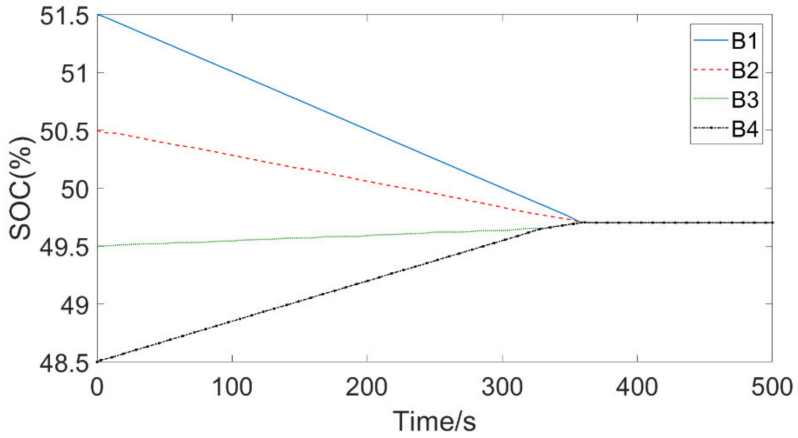

Figure 4. Simulation of cascaded Buck-Boost balance circuit based on fuzzy control.

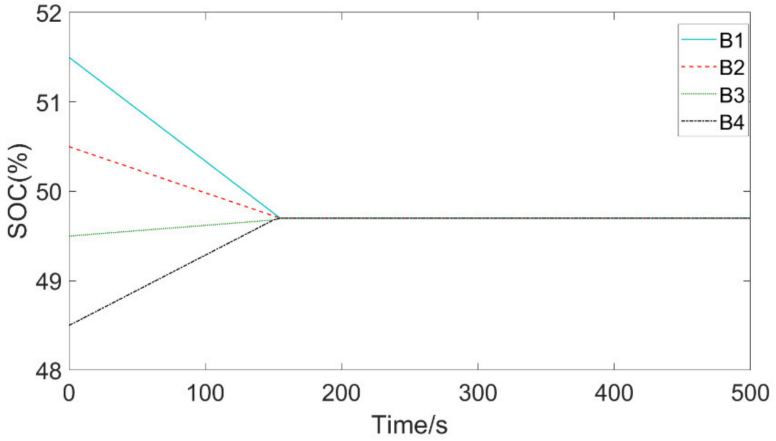

Figure 5. Simulation of cascaded Buck-Boost balance circuit based on MPC.

The MPC algorithm and simulation model are built according to each parameter index. The parameters of the MPC algorithm are described as follows.

$$A = \begin{bmatrix} 1 & 0 & 0 & 0 \\ 0 & 1 & 0 & 0 \\ 0 & 0 & 1 & 0 \\ 0 & 0 & 0 & 1 \end{bmatrix}, B = \begin{bmatrix} -1 \times 10^{-5} & 0 & -5 \times 10^{-6} \\ 1 \times 10^{-5} & 0 & -5 \times 10^{-6} \\ 0 & -1 \times 10^{-5} & 5 \times 10^{-6} \\ 0 & 1 \times 10^{-5} & 5 \times 10^{-6} \end{bmatrix}, x_0 = \begin{bmatrix} 0.9 \\ 0.8 \\ 0.7 \\ 0.6 \end{bmatrix}, Q = \begin{bmatrix} 1 & 0 & 0 & 0 \\ 0 & 1 & 0 & 0 \\ 0 & 0 & 1 & 0 \\ 0 & 0 & 0 & 1 \end{bmatrix}, R = \begin{bmatrix} 1 & 0 & 0 \\ 0 & 1 & 0 \\ 0 & 0 & 1 \end{bmatrix}.$$

The simulation results show that before the balance starts, $SOC_{max} - SOC_{min} = 3\%$. The remaining power of each cell with large differences in the initial state gradually converges during the balance process. From the simulation time analysis, when the balance time is T = 358, the SOC of the cascaded Buck-Boost balance circuit based on fuzzy control is highly consistent, and the balance stops; and in the cascaded Buck-Boost balance circuit based on model prediction control, when the balance time is T = 151 s, the SOC of the four batteries in series reaches a high degree of consistency, and the balance is over. At this time, both algorithms can enable the system to achieve the desired goal of balance. From the simulation effect analysis, the balance scheme based on model predictive control can flexibly estimate the balance current and then accurately control the duty ratio of MOSFET. The single battery does not repeatedly charge and discharge, the balance curve is well fitted, and the balance efficiency and speed meet the expected indicators.

From the balance efficiency analysis, at the beginning of the balance, the SOC of the series battery pack is displayed according to the average value of the SOC of the cells in this group. Due to the 'bucket effect', the available capacity of the four-cell battery is determined by the cell with the lowest energy. At this time, the actual SOC is 48.5% and the actual available capacity is 1261 mAh, resulting in the driver being unable to accurately provide the remaining battery power. After the cascaded Buck-Boost balance circuit based on fuzzy control, the SOC = 49.7%, the available capacity is 1292.2 mAh, and finally the available capacity is increased to 31.2 mAh. After the cascaded Buck-Boost balance circuit based on model predictive control, the SOC = 49.66% and the available capacity is 1291.16 mAh, with a final boosted available capacity of 30.16 mAh.

Under the condition that the balance efficiency is basically the same, the cascaded Buck-Boost balance circuit based on model prediction control has a significantly faster balance speed and is more suitable for the actual working process.

Combined with the simulation circuit, the schematic diagram of the balance circuit is designed. As shown in Figure 6, the MOS tube with small conduction impedance and a large working voltage and current—IRF3205—is selected. According to the conduction voltage drop and the maximum freewheeling requirements, we selected a 16 CTQ100 diode. Through the TLP250 optocoupler isolation of the power circuit and control circuit, we effectively avoid interference from the power circuit to the control loop; the selected magnetic ring inductor has an operating current up to 2 A, which can efficiently store energy to achieve energy transfer. The model predictive control was transplanted to STM32 to complete the equilibrium experiment.

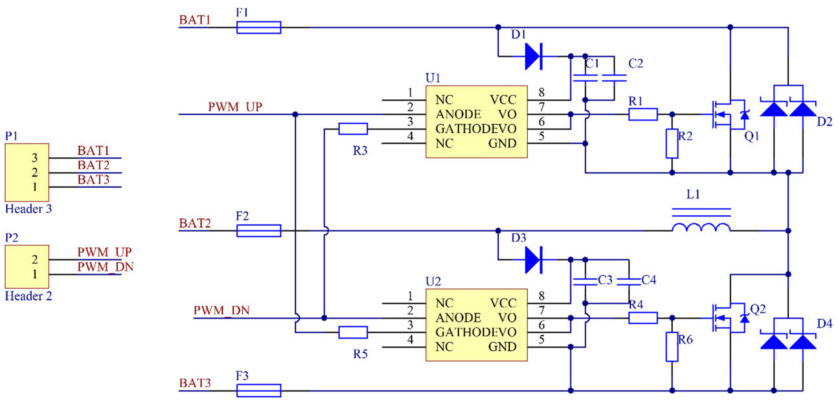

Figure 6. Hardware schematic of the balanced circuit.

To further verify the flexibility and accuracy of the cascade active balance method based on model prediction control, several possible inconsistencies are simulated. That is, the inconsistencies in different SOC stages, the uniformity of SOC differences between any monomers, and the non-uniformity of SOC differences between any monomers. The specific simulation is shown in Figure 7.

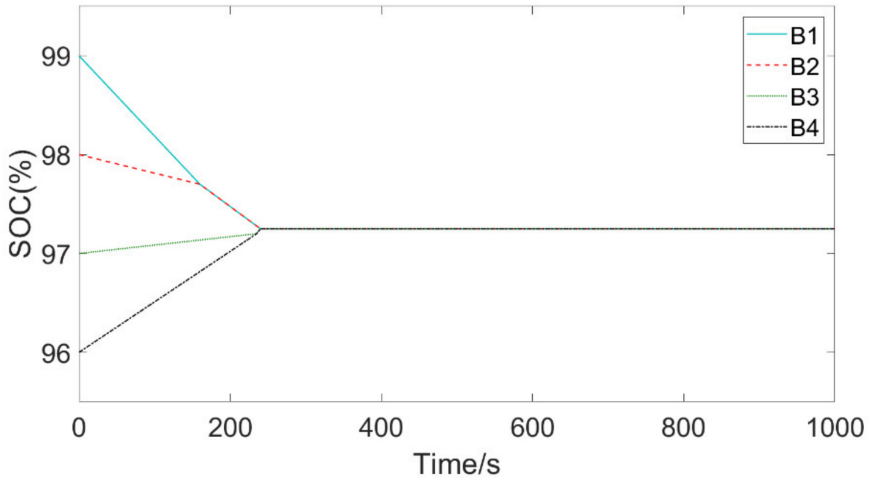

(**a**)

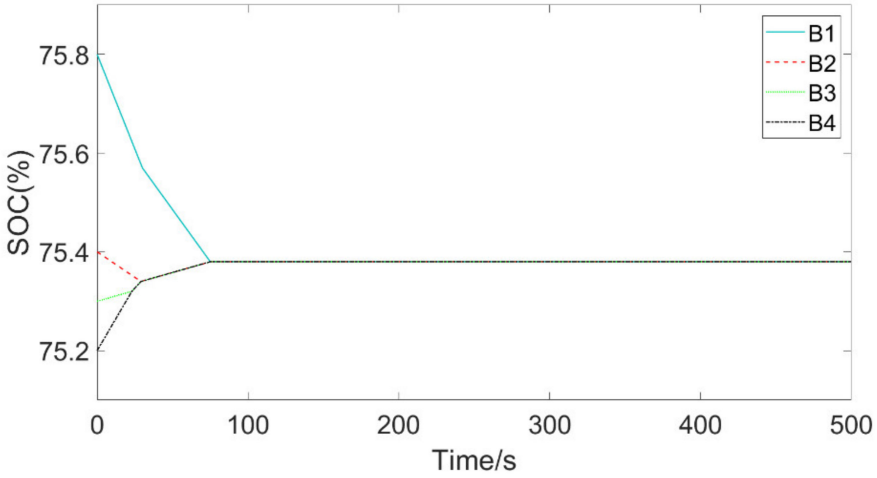

(**b**)

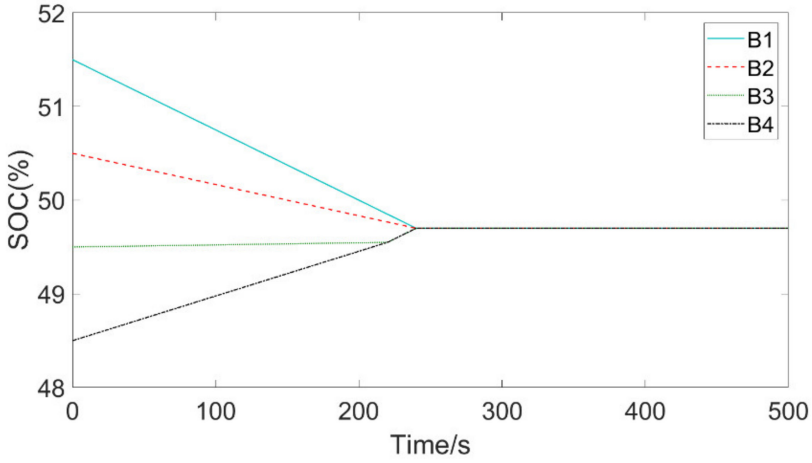

(**c**)

Figure 7. *Cont.*

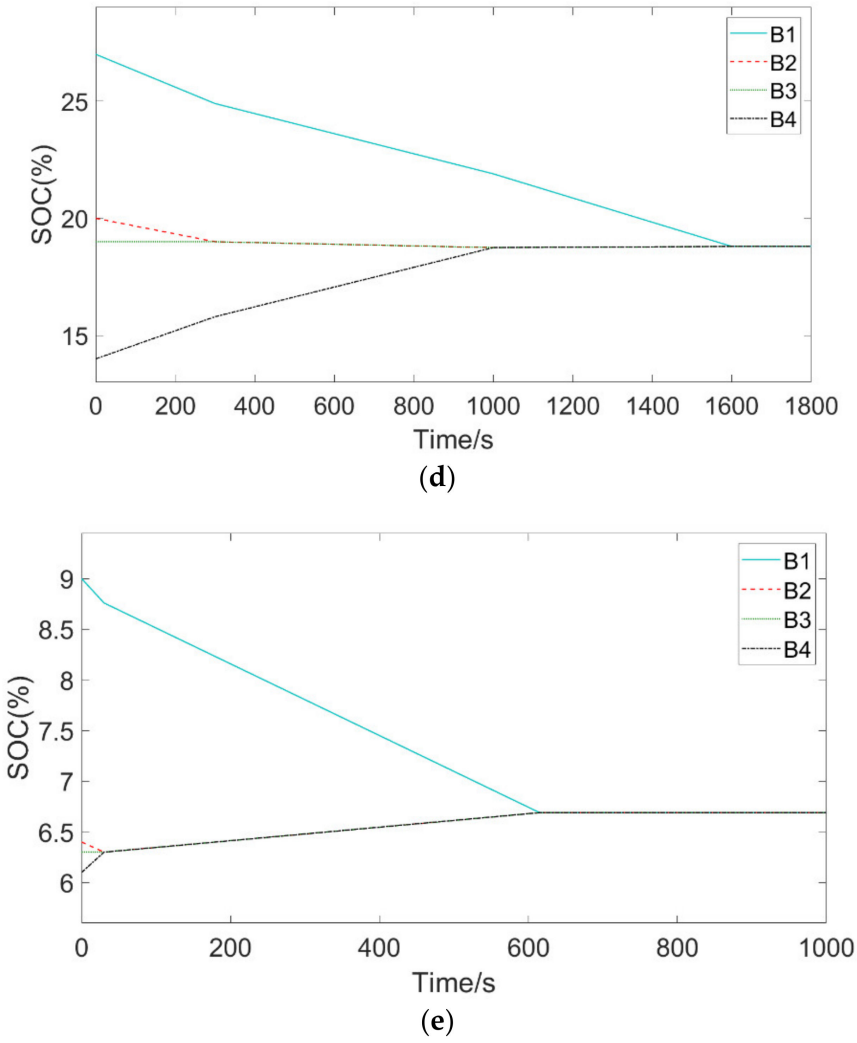

Figure 7. Battery SOC curve at different states of balance.

Figure 7a–e said the battery under the MPC from different SOC to balanced and consistent. In order to further describe the equilibrium process in the experiment, the SOC range before the balance was set as SOCmax-SOCmin and the average SOC of the series battery pack was $\overline{SOC}$. The balance results under different states are shown in Table 3.

Table 3 shows the comparison of the battery pack information before and after balancing for the five groups of inconsistent batteries at rest. It can be found that the maximum SOC difference among the listed cells is 13% and the minimum is 0.6%. The size of the difference affects the balance speed: the smaller the difference, the faster the balance speed, and vice versa. At the same time, the larger the range, the more the battery capacity can be improved after the balance; the smaller the range, the less the battery capacity can be improved after equilibrium. The balance control method designed in this paper can efficiently improve battery pack inconsistency in different states, effectively improve battery pack capacity utilization, extend range, and increase battery life.

Table 3. Battery balance results under different states.

Battery State		Battery SOC (%)						Time (s)	Useful Capacity (mAh)	Increasing Capacity (mAh)
		Battery 1	Battery 2	Battery 3	Battery 4	Range	Mean			
a	Before balanced	99	98	97	96	3	97.5	237	2496	32.708
	After balanced	97.261	97.259	97.259	97.155	0.006	97.258		2528.708	
b	Before balanced	75.8	75.4	75.3	75.2	0.6	75.425	72	1955.2	4.42
	After balanced	75.374	75.37	75.37	75.368	0.006	75.37		1959.62	
c	Before balanced	51.5	50.5	49.5	48.5	3	50	233	1261	30.42
	After balanced	49.67	49.67	49.67	49.67	0	49.67		1291.42	
d	Before balanced	27	19	19	14	13	20	1618	364	122.72
	After balanced	18.723	18.72	18.72	18.718	0.005	18.72		486.72	
e	Before balanced	9	6.4	6.3	6.1	2.9	6.95	625	158.6	14.04
	After balanced	6.642	6.640	6.640	6.638	0.004	6.64		172.64	

5. Conclusions

In this paper, aiming at the deficiency that the traditional balance topology can only balance two adjacent single cells, an improved balance topology is designed, and model prediction control is used as the balance control strategy to control the MOSFET duty cycle in the balance circuit. By building a simulation model and actual balance circuit on the Simulink platform, the balance circuit and control strategy designed in this paper are verified theoretically and experimentally. The results show that model prediction control reduced the balance time by 207 s compared with the fuzzy control algorithm, reaching the same balance value with a maximum error of 3% in the SOC. Moreover, the improved Buck-Boost balance topology based on model prediction control increased the available capacity of the battery by 122.72 mAh when the maximum SOC difference of the four batteries was 13% and the minimum SOC difference was 0.6%. Compared with the fuzzy control method, this method is faster, effectively improves the available capacity of the battery pack, and prolongs the battery range and service life.

In this study, external factors (such as the ambient temperature and humidity of the working battery) may have affected the efficiency of the balanced battery, but this paper gave priority to the influence of battery working current and working voltage—the two most important factors for balance efficiency. The subsequent work will gradually take into account the influence of external factors on balance efficiency. An electric vehicle drives in a complex and dynamic "human-vehicle-road" closed-loop system, and it is difficult to meet the needs of modern intelligent electric-vehicle technology to balance power battery control with a fixed control strategy. This will be the main direction of this paper's future work: to balance the battery pack with the driver's intention, vehicle condition and road condition data obtained from online intelligent identification, and to realize the optimal management of battery packs under different operating conditions under the unified framework of "person-vehicle-road".

Author Contributions: Conceptualization, Q.W.; methodology, Q.W.; software, T.G.; validation, Q.W. and C.W.; investigation, T.G.; resources, X.L. and C.W.; data curation, Q.W.; writing—original draft preparation, X.L.; writing—review and editing, Q.W. and X.L.; visualization, X.L. and C.W.; supervision, T.G.; project administration, Q.W.; funding acquisition, Q.W. All authors have read and agreed to the published version of the manuscript.

Funding: This research received no external funding.

Institutional Review Board Statement: Not applicable.

Informed Consent Statement: Not applicable.

Data Availability Statement: Not applicable.

Conflicts of Interest: The authors declare no conflict of interest.

References

1. Yang, F.; Wang, D.; Zhao, Y.; Tsui, K.L.; Bae, S.J. A study of the relationship between coulombic efficiency and capacity degradation of commercial lithium-ion batteries. *Energy* **2018**, *145*, 486–495. [CrossRef]
2. Kwon, S.-J.; Lee, S.-E.; Lim, J.-H.; Choi, J.; Kim, J. Performance and Life Degradation Characteristics Analysis of NCM LIB for BESS. *Electronics* **2018**, *7*, 406. [CrossRef]
3. Ali, M.; Zafar, A.; Nengroo, S.; Hussain, S.; Kim, H. Effect of Sensors Sensitivity on Lithium-Ion Battery Modeled Parameters and State of Charge: A Comparative Study. *Electronics* **2019**, *8*, 709. [CrossRef]
4. Go, S.-I.; Choi, J.-H. Design and Dynamic Modelling of PV-Battery Hybrid Systems for Custom Electromagnetic Transient Simulation. *Electronics* **2020**, *9*, 1651. [CrossRef]
5. Luo, W.; Jie, L.; Song, W.; Feng, Z. Study on passive balancing characteristics of serially connected lithium-ion battery string. In Proceedings of the 13th International Conference on Electronic Measurement & Instruments, Yangzhou, China, 20–22 October 2017. [CrossRef]
6. Zheng, Y.; He, F.; Wang, W. A Method to Identify Lithium Battery Parameters and Estimate SOC Based on Different Temperatures and Driving Conditions. *Electronics* **2019**, *8*, 1391. [CrossRef]
7. Carter, J.; Fan, Z.; Cao, J. Cell equalization circuits: A review. *J. Power Sources* **2020**, *448*, 227489. [CrossRef]
8. Xu, X.; Xing, C.; Wu, Q.; Qian, W.; Zhao, Y.; Guo, X. An Active State of Charge Balancing Method with LC Energy Storage for Series Battery Pack. *Front. Energy Res.* **2022**, *10*, 1811. [CrossRef]
9. Sahoo, J.; Ramesh, P.; Patra, A. Interleaved Operation of Conventional PWM Control in a Buck-Boost Active Balancing Circuit. In Proceedings of the 2020 IEEE International Conference on Power Electronics, Drives and Energy Systems (PEDES), Jaipur, India, 16–19 December 2020. [CrossRef]
10. Zhang, Y.; Yang, R. An Improved Buck-Boost Circuit Equalization Method for Series Connected Battery Packs. In Proceedings of the 2021 IEEE 4th International Electrical and Energy Conference (CIEEC), Wuhan, China, 28–30 May 2021. [CrossRef]
11. Yang, Z.-Z. Development of an Active Equalizer for Lithium-Ion Batteries. *Electronics* **2022**, *11*, 2219. [CrossRef]
12. Wu, T.; Qi, Y.; Liao, L.; Ji, F.; Chen, H. Research on equalization strategy of lithium-ion batteries based on fuzzy logic control. *J. Energy Storage* **2021**, *40*, 102722. [CrossRef]
13. Liao, L.; Chen, H. Research on two-stage equalization strategy based on fuzzy logic control for lithium-ion battery packs. *J. Energy Storage* **2022**, *50*, 104321. [CrossRef]
14. Wu, T.; Chen, L.; Xu, Y.; Zhang, X. Balancing method of retired battery pack based on variable domain fuzzy control. *J. Electrochem. Energy Convers. Storage* **2023**, *20*, 041005. [CrossRef]
15. Wang, B.; Qin, F.; Zhao, X.; Ni, X.; Xuan, D. Equalization of series connected lithium-ion batteries based on back propagation neural network and fuzzy logic control. *Int. J. Energy Res.* **2020**, *44*, 4812–4826. [CrossRef]
16. Wang, B.; Xuan, D.; Zhao, X.; Chen, J.; Lu, C. Dynamic battery equalization scheme of multi-cell lithium-ion battery pack based on PSO and VUFLC. *Int. J. Electr. Power Energy Syst.* **2022**, *136*, 107760. [CrossRef]
17. Wang, Y.-X.; Zhong, H.; Li, J.; Zhang, W. Adaptive estimation-based hierarchical model predictive control methodology for battery active equalization topologies: Part II-equalizer control. *J. Energy Storage* **2022**, *45*, 102958. [CrossRef]
18. Hoque, M.M.; Hannan, M.; Mohamed, A. Optimal algorithms for the charge equalisation controller of series connected lithium-ion battery cells in electric vehicle applications. *IET Electr. Syst. Transp.* **2017**, *7*, 267–277. [CrossRef]

Disclaimer/Publisher's Note: The statements, opinions and data contained in all publications are solely those of the individual author(s) and contributor(s) and not of MDPI and/or the editor(s). MDPI and/or the editor(s) disclaim responsibility for any injury to people or property resulting from any ideas, methods, instructions or products referred to in the content.